Journal of Nuclear Materials 482 (2016) 229–235

Contents lists available at ScienceDirect

Journal of Nuclear Materials

journal homepage: www.elsevier.com/locate/jnucmat

Sequestration of radioactive iodine in silver-palladium phases in commercial spent nuclear fuel

Edgar C. Buck*, Edward J. Mausolf, Bruce K. McNamara, Chuck Z. Soderquist, Jon M. Schwantes

Pacific Northwest National Laboratory, P.O. Box 999, Mail Stop P7-27, Richland, WA 99352, United States

HIGHLIGHTS

- A Pd-Ag halide phase has been observed in a high burn-up UO_2 reactor fuel.
- The phases contains iodine and bromine.
- Iodine release in high burnup fuels may be reduced through the formation of recalcitrant phases.

ARTICLE INFO

Article history:
Received 23 May 2016
Received in revised form
14 October 2016
Accepted 17 October 2016
Available online 19 October 2016

Keywords:
AgI
Fuel dissolution
Scanning electron microscopy
Energy dispersive x-ray spectroscopy
Elemental mapping

ABSTRACT

Radioactive iodine is the Achilles' heel in the design for the safe geological disposal of spent uranium oxide (UO_2) nuclear fuel. Furthermore, iodine's high volatility and aqueous solubility were mainly responsible for the high early doses released during the accident at Fukushima Daiichi in 2011. Studies Kienzler et al., however, have indicated that the instant release fraction (IRF) of radioiodine ($^{131/129}I$) does not correlate directly with increasing fuel burn-up. In fact, there is a peak in the release of iodine at around 50–60 MW d/kgU, and with increasing burn-up, the IRF of $^{131/129}I$ decreases. The reasons for this decrease have not fully been understood. We have performed microscopic analysis of chemically processed high burn-up UO_2 fuel (80 MW d/kgU) and have found recalcitrant nano-particles containing, Pd, Ag, I, and Br, possibly consistent with a high pressure phase of silver iodide in the undissolved residue. It is likely that increased levels of Ag and Pd from ^{239}Pu fission in high burnup fuels leads to the formation of these metal halides. The occurrence of these phases in UO_2 nuclear fuels may reduce the impact of long-lived ^{129}I on the repository performance assessment calculations.

1. Introduction

Light water nuclear reactor fuels used in commercial power plants consist of uranium oxide (UO_2) and/or mixed oxide $(U,Pu)O_2$ ceramic pellets contained within zirconium alloy cladding [1–6]). Once irradiated to burn-ups exceeding 50–60 MWd/kgU, the spent nuclear fuel (SNF) undergoes significant chemical and microstructural changes [1]. Fission products, such as Zr, Sr, and the lanthanides, as well as the neutron capture products; Pu, Np, and Am, are retained in the UO_2 (uraninite) fluorite-type structure. The fission gases, Xe and Kr, are trapped as gas bubbles and the transition metals (Mo, Tc, Ru, Rh, and Pd) are partitioned into metallic phases that are found embedded in the fuel grains, grain boundaries, defects, and triple points [4–8]. Smaller amounts of Ag, Te, and Se are also thought to be associated with these phases, although Ag is almost completely immiscible in Ru metal [9]. Iodine has been assumed to form CsI, the most favorable sites being at fission-gas bubbles, grain boundaries, and cracks in the matrix. At low burn-ups (<5 MWd/kgU), CsI is not expected to form; however, at higher burnups, the radiation-induced bubble microstructure is thought to serve as reaction sites for thermodynamically favorable CsI formation [2,10]. As the Cs/I molar ratio is ~10, excess cesium forms Cs_2MoO_4. Thomas et al. [4] reported the occurrence of Ag-Pd precipitates in SNF using Auger spectroscopy.

Knowledge of the distribution of radionuclides partitioning between the fuel matrix and other discrete phases within or outside the fuel grains is necessary to make predictions about potential release if the fuel bundle is compromised in some manner.

* Corresponding author.
E-mail address: edgar.buck@pnnl.gov (E.C. Buck).

http://dx.doi.org/10.1016/j.jnucmat.2016.10.029
0022-3115/

For instance, a fraction of the inventory of fission gases and some of the more volatile radioelements (e.g., Cs, I) may migrate out of the UO_2 matrix during in-reactor operations and accumulate in locations, collectively referred to as the "gap region" (e.g., the interface between the pellets and the cladding, the rod plenum regions, and pellet fracture surfaces) [1–3].

Nuclear accidents that have resulted in melting or partial melting of the reactor core have led to the rapid release of these volatile radionuclides, many of which have short half-lives and contribute to hazardous dose levels [10,11]. Radioactive iodine-131 ($t_{1/2} = 8$ d) is one of the most harmful radionuclides because it has the highest activity among radionuclides that could be released after an accident. During the Chernobyl accident in 1986, 30–40% of the ^{131}I was released, contributing to approximately 17–45 MCi; and during the Fukushima Daiichi accident in 2011, ~0.03 MCi of ^{131}I was released. There is interest in understanding the release of this radionuclide, as such information may provide insight into the fuel condition at the time of the accident [12–16].

Iodine (^{131}I) is the radioisotope of concern for accident scenarios but it is not an issue for either long-term storage or fuel recycling, owing to its rapid decay. However, another iodine radioisotope, ^{129}I ($t_{1/2} = 15.5$ Ma), becomes a concern at the time-scale of potential reprocessing (or recycling) operations, storage, and final geologic disposal. A nuclear fuel reprocessing facility, such as La Hague in France that is capable of handling ~1400 t of SNF per year, might process ~320 kg of ^{129}I each year. The difficulty of retaining ^{129}I during recycle is one of the major factors that hinders the development of fuel recycling world-wide [17]. Because ^{129}I is assumed to be released instantly from a compromised SNF waste package, it plays a significant role in performance assessment calculations for geologic disposal under all repository designs. Data from Gray [18] and Finn and coworkers [19] have illustrated a clear relationship between fission gas release (FGR) and the release of several radionuclides, including radioiodine; although, it should be noted that the FGR does not necessarily correlate with fuel burnup. At higher burn-ups, there has been tentative evidence of radioiodine retention during fuel dissolution. Kienzler and González-Robles have pointed out that linear power is a much better predictor of iodine release than burnup [20].

In this paper, we show, for the first time, in high burn-up SNF, that iodine is sequestered into a solid phase. This phase could limit the subsequent release of iodine under geologic disposal in an engineered repository, during fuel recycle operations (depending on the chemical processes used), or possibly, during a nuclear accident event.

Initial characterization of Approved Testing Material (ATM)-109, a spent fuel from a Boiling Water Reactor from the Quad Cities I reactor (Quad Cities Generating Station, Cordova, Illinois, USA) was performed by Wolf et al. [21]. This fuel was irradiated from February 1979 to September 1987, and again from November 1989 to September 1992. The original uranium oxide (UO_2) fuel was fabricated by the General Electric Company. The UO_2 had an initial 3.0% ^{235}U enrichment and an initial grain size of ~30 μm. The specimens received a maximum burn-up of 70–80 MWd/kgU. This higher burn-up resulted in more ^{239}Pu fission and the SNF possessed higher levels of Ag than lower burn-up fuels. We have previously reported on the nature of the metallic epsilon particles from these fuels and aspects of their chemistry [22,23]. Palomares and co-workers [24] reported on the composition of undissolved residues from the dissolution of ATM-109 fuel using concentrated nitric acid (CNA) and ammonium carbonate-peroxide (ACP) dissolution methods. These ACP and CNA dissolution processes have been described elsewhere in detail [25–27]. The neutron activation results reported by Palomares and co-workers indicated that the CNA dissolved fuel had a slightly lower Mo and Ru concentration than the ACP dissolved material and that the residue material from the ACP process contained far more radioiodine (700% more) than the CNA dissolved material [24]. Results for Br, Ag and Pd were not reported in the neutron activation study.

In this paper, we report the direct observation of iodine associated with Ag and Pd in SNF. The object of this paper is to provide evidence for the occurrence of this material in the undissolved solids and then to discuss its origin as either in the original SNF or whether this material formed during the CNA and ACP dissolution processes.

2. Experimental section

As of July 2014, the ATM-109 fuel had been cooling for approximately 22 years. The material was dissolved using two dissolution solutions; hot concentrated nitric acid (termed CNA) and ammonium carbonate-peroxide (ACP). The dissolution process that produced the samples examined in this paper is described in detail in Refs. [25,26]. However, in summary, the fuel was dissolved using the following process: 12.0536 g of raw UO_2 fuel, crushed to pass through a 212-μm screen, was dissolved in a saturated solution of ammonium carbonate with about one fifth its volume of 30% H_2O_2, at room temperature and atmospheric pressure. The reaction was continued for four days, leaving the noble metal phase as a fine black suspension. The black suspension was filtered out of solution using a 0.45-μm membrane filter. The filtrate was clear yellow. The black suspension was then treated with more ammonium carbonate, hydrogen peroxide solution to assure that the UO_2 had completely dissolved. No further yellow color appeared in the solution, indicating that no more uranium was going into solution. The black insoluble matter was washed with 0.5 M HNO_3 to dissolve the soluble carbonates (expected $BaCO_3$ and $SrCO_3$), then centrifuged. The washed black solids were dried and weighed. Final dry weight of black insoluble matter (consisted largely of noble metal phase) was 0.2320 g.

Each of these treatments dissolved the UO_2 and nearly all of the fission products and transuranic elements, leaving an undissolved residue of fine, black material that consisted largely of the metals; Mo, Tc, Ru, Rh, and Pd, and with smaller amounts of other elements. Approximately 13 g of fuel was used for each dissolution. The black undissolved residue was centrifuged out of solution, washed to remove the dissolved fuel, and then removed from the hot cell for analysis.

2.1. Sampling

The undissolved solids recovered from these treatments of the ATM-109 were slurried in water and placed in polyethylene vials. Aliquots were pipetted from these slurries onto carbon coated TEM grids and SEM mounts.

2.2. Microanalysis with SEM and TEM

Specimens of the undissolved SNF residues were carefully removed from the parent sample under radiologically protected environments (i.e. radioactive materials glove box) and transferred to smaller vials. For scanning electron microscopy (SEM) analysis, these vials were opened in a contained chamber and a few particles were placed on a clean glass slide. A pipette containing a small amount of methanol was used to extract a few particles. These were then deposited on a sticky carbon tape, coated with conductive carbon and analyzed with an FEI (Hillsboro, OR, USA) Quanta250™ field emission gun SEM equipped with an EDAX (EDAX Inc., Mahwah, NJ) compositional analysis system. Images were obtained under backscattered electron (BSE) imaging conditions and

elemental x-ray maps were also collected. X-ray maps were collected over 24–72 h with the aid of drift-correction software. The elemental maps were reported as (red-green-blue) RGB combination images of three selected elements (I, Ag, and Pd). Image fusion techniques were employed using plugin programs available from ImageJ [27]. These elements were present at low levels in the specimen compared to the major epsilon phase elements (Mo, Ru, and Tc); and hence, this combination of elemental maps allowed clear observation of the minor features of interest. Spot analyses were also performed to obtain the composition of the solids; however, these were subject to the available probe size.

The samples were examined further with a FEI Tecnai™ T30 Transmission Electron Microscope (TEM) operated at 300 keV. The TEM was equipped with an EDAX x-ray energy dispersive spectrometer and a Gatan Orius™ digital camera. The magnification and camera lengths were checked against a MAG*I*CAL silicon standard [28]. Diffraction patterns and electron micrographs were analyzed with Gatan DigitalMicrograph™ 1.83.842 and custom scripts by Mitchell [29]. Simulated diffraction patterns were generated using CrystalMaker®2.2, a crystal and molecular structures program for Mac and Windows, and SingleCrystal®2.0.1, an electron diffraction simulation program distributed by CrystalMaker Software Ltd., Oxford, England (http://www.crystalmaker.com). EDS spectra were modeled and compared to experimental data using DTSA-II software [30].

3. Results

The residue solids in Fig. 1a and b shows SEM images of the material at two different magnifications from the ACP dissolution of ATM-109. The large majority of the material was the 5-metal (Mo-Tc-Ru-Rh-Pd), epsilon phase and consisted of agglomerates of much smaller particles. The nature of this material has been reported in detail elsewhere [22]. Fig. 1c and d shows the elemental mapping analysis of residue material from the regions shown in Fig. 1a and b, respectively. There was clear evidence for the occurrence of minor phases in addition to the major 5-metal phase which is represented by the dominant blue coloration in the elemental distribution maps. By combining the elemental maps of iodine, Ag, and Pd as RGB images, two minor phases were revealed. The yellow-green material was consistent with a silver-iodide phase and the orange was more consistent with a palladium-iodide phase, based on the mixing color triangle (insert). Spot analyses were then employed to determine the composition of the iodine-bearing phase. In Fig. 2, elemental spot analysis of different regions of the specimen (Fig. 2a) revealed the dominant 5-metal composition and an AgI composition, as well as compositions that were mixtures (see Fig. 2b). There was also evidence for the presence of Pd in the AgI phase (see Table 1 for measured composition of the particles obtained with EDS as well as the literature characteristic x-ray energies for the major elements compared to experimentally obtained values in this study). The higher energy x-ray lines shown minor amounts of uranium (U-L line) in the 5-metal phase and the absence of this element in the Ag-rich phase (see Fig. 2c). There was overlap of the signals due to the proximity of the phases. The darker-looking solid in The concentration of iodine in the ACD process was known to be higher in the undissolved solids than in the CNA process based on the investigations by Palmores et al. [24]. However, once, SEM mapping had revealed the presence of discrete iodine-bearing phases, an attempt was made to locate similar iodine-containing phases in the nitric acid dissolved specimens. In Fig. 3a, an SEM image of the residue solids resulting from the dissolution of the ATM-109 fuel in CNA process is shown. This region was shown to contain iodine. It possessed a distinctly different

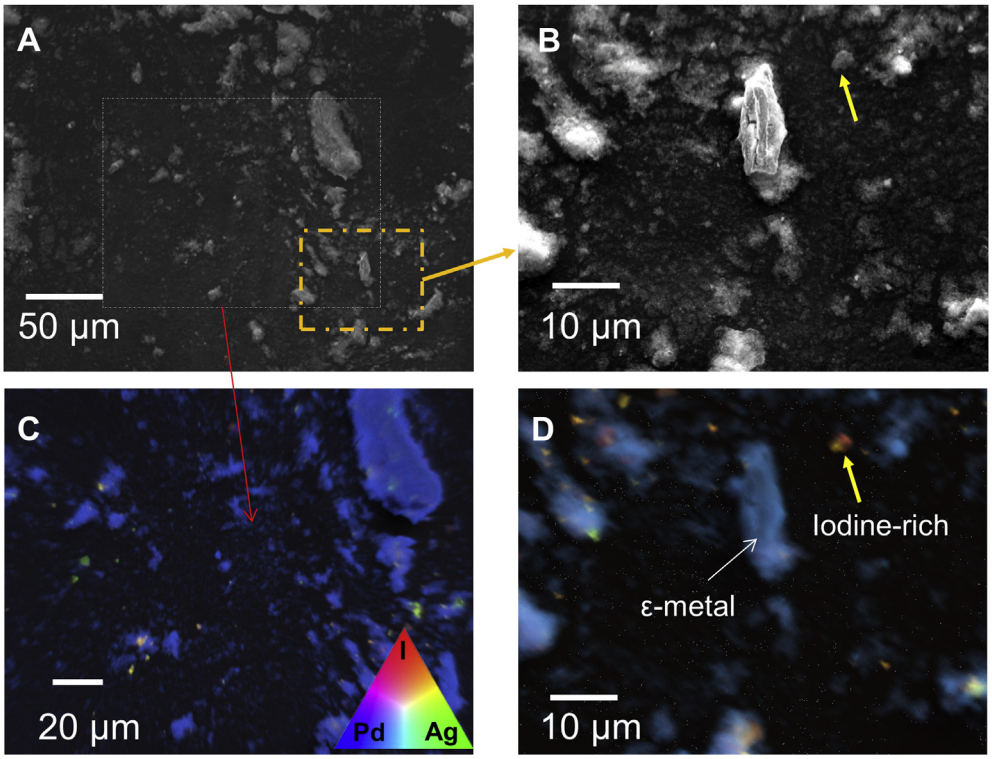

Fig. 1. (**a**) SEM-BSE image of solid residues from ammonium carbonate-peroxide dissolution, (**b**) higher magnification SEM-BSE image of this area and the corresponding combination elemental maps (**c** and **d**) showing the occurrence of an ($AgI:PdI_2$) phase (orange colored regions) and silver areas (green). (For interpretation of the references to colour in this figure legend, the reader is referred to the web version of this article.)

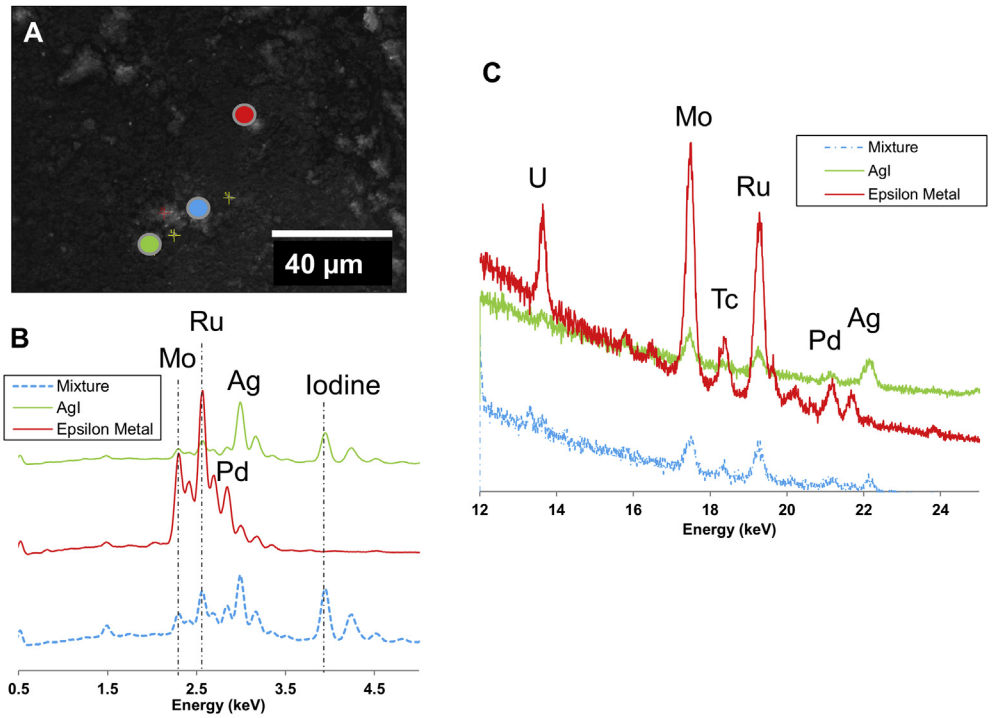

Fig. 2. (**a**) SEM-BSE image of undissolved solid residues, (**b**) low energy lines from the EDS analysis of different regions showing the occurrence of a AgI phase as well as a composition consistent with the 5-metal phase, and (**c**) high energy-portion of the EDS analysis showing the K-lines from Mo, Tc, Ru, and Pd from the metallic phase and a silver-iodide phase.

Table 1
Results from EDS analyses of the halide-rich particles using quantitative data from simulation.

Element	Measured Energies (keV)	Literature Energies (keV)	Element Mass %
I	3.93	3.937	49.7
Br	11.90	11.924,11.877	3.1
Mo	17.48	17.479	0.4
Ru	19.23	19.279	0.4
Pd	21.11	21.163	4.2
Ag	22.12	22.177	42.2

contrast to the more common 5-metal residue material; however, under secondary electron imaging, these areas looked very similar. In Fig. 3b, combination elemental mapping using elemental distribution maps from iodine, Ag, and Pd of the CNA dissolution process residue is shown. In this specimen, the iodine-containing particles were frequent, less obvious, and were more difficult to locate than in the ACP dissolved material, but there was evidence for an iodine-bearing phase. The observation of iodine phases in the nitric acid material is in full agreement with the findings of Palmores et al. [24]. An effort was made to locate the same phases in the TEM using conventional bright field imaging. However, with the TEM, additional evidence for a halide phase was found (see Fig. 4a and b) only in one instance. This particular phase contained more Pd than Ag. We were unable to locate other examples of the

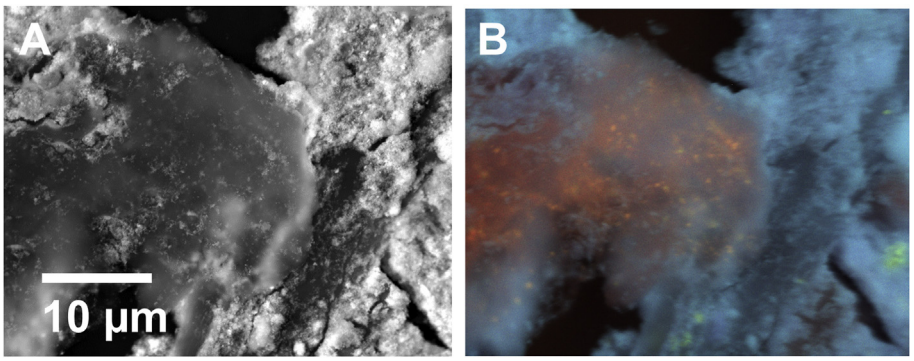

Fig. 3. (**a**) SEM-BSE image of residues dissolved in concentrated nitric acid, (**b**) and the corresponding combination elemental map showing the occurrence of (Ag,Pd) halide phases (orange-colored regions) interspersed within the epsilon metal (bluish), and silver (bright green). (For interpretation of the references to colour in this figure legend, the reader is referred to the web version of this article.)

iodine phase during the TEM investigation. A more thorough STEM-HAADF investigation is warranted of the material that could target the phases of interest.

Bromine is a minor fission product that is present at <10% of the iodine level in these fuels. However, during the analysis of the iodine phase, a peak suggesting the presence of Br was detected. We believe that this is the first reported detection of Br in a spent nuclear fuel using electron microscopy (Fig. 5). The Br signal was clearly evident from peaks at 11.64 and 12.95 keV (see Table 1). The Br x-ray lines were measured at 11.90 keV (major) and 13.27 keV (minor) and these compared well to literature values $K\alpha_1$ and α_2 lines at 11.924 and 11.877 keV, respectively and the $K\beta_1$ line at 13.29 keV. The spectrum matched well to a calculated spectrum using DTSA-II [30]. The mixed AgI:PdI_2 phase in the nuclear fuel was found to be less beam sensitive than a standard specimen of AgI; however, the electron diffraction pattern were consistent with a pure cubic AgI phase. The EDS elemental analysis of the phase in the TEM showed that it contained much more Pd than Ag (see Fig. 4b). The association of Ag and Pd in the phase suggests that this phase is good evidence that it was present in the original undissolved fuel.

4. Discussion

If water enters a geologic waste repository containing SNF rods with breached cladding, the soluble radionuclides, including iodine and cesium, would be expected to quickly dissolve [1]. Laboratory

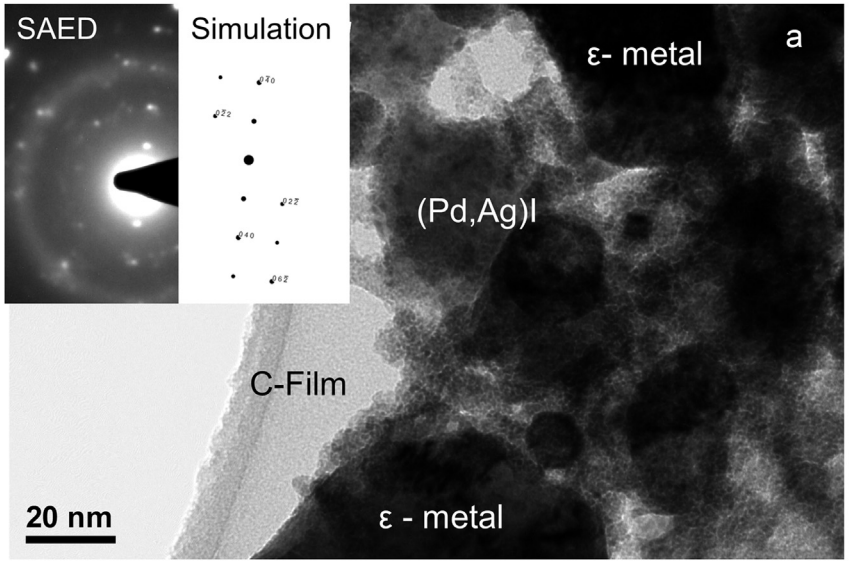

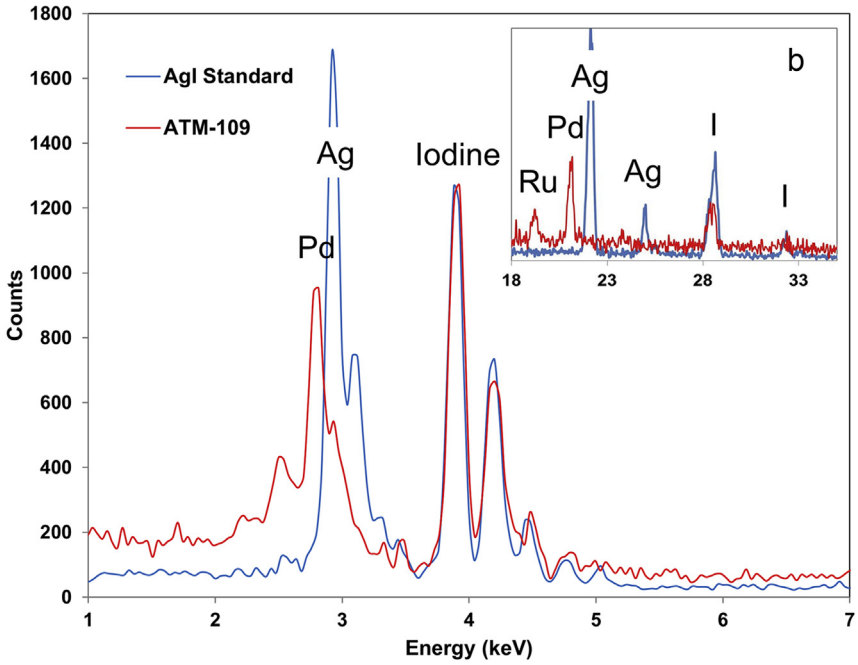

Fig. 4. **(a)**. TEM image of undissolved solid residues showing the occurrence of a mixed (AgI:PdI_2) phase with the selected area electron diffraction pattern and simulation showing a systematic row along the [010] direction (insert) consistent with cubic AgI (**a** = 6.43 Å). **(b)**. TEM-EDS analysis of the halide phase showing the co-precipitation of Pd in this phase. The variation in the Pd-Ag ratio in the halide phase is supportive that these phases did not form during chemical dissolution of the ATM-109 nuclear fuel but were rather present in the original fuel. The variability can be explained by different neutron fluxes through the fuel pellet that resulted in higher concentrations of Ag in some areas and higher concentration of Pd in others.

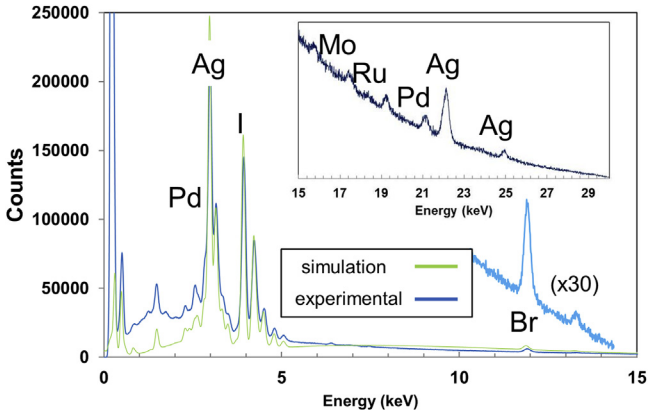

Fig. 5. SEM-EDS analysis of AgI phase showing the presence of Br and Pd in the phase and DTSA II simulation spectrum showing the AgI phase. The intensity between 10 and 14 keV has been multiplied to reveal the Br. The insert shows the spectra from 15 keV to 30 keV and shows, lower levels of Mo, Ru, as well as the Pd and Ag signals.

measurements of a few low burnup SNF materials show that the measured combined grain inventories and grain boundary inventories of ^{129}I were approximately equal to the fission gas release fractions [18,19]. In these fuels, the majority of the iodine has migrated, together with Cs, to grain boundaries, fractures, and gaps in the fuel and fuel-cladding regions [11,12]. However, in high burnup fuels, there is apparent retention in iodine [20,24], until now the mechanism of this retention was unknown. The assumption based on thermodynamic arguments and microstructural analyses from Kleykamp [2,3] and Grimes et al. [31] is that iodine forms CsI precipitates in irradiated UO_2 fuels. Computational models by Middleburgh et al. [32] examined the drivers for the incorporation of fission products including noble gases Kr and Xe, and Cs and iodine, as well as metallic products Te, Sn, Cd, and Ag into the 5-metal, epsilon phase in nuclear fuels with increasing burn-up. The solution and accommodation energies for Cs, Xe, and Kr were such that incorporation would not occur even if injected via radiation processes into the metal, in agreement with the microanalysis findings of Thomas et al. [4]. The calculations did show that in the absence of Cs, iodine may be retained in Mo-rich epsilon phases but in low Mo content epsilon phases, iodine will be driven from the phase. Mo content decreases with increasing burn-up and this may provide a mechanism for the formation of the Ag or Pd iodide.

In this study, micro-analysis of the residue from dissolved ATM-109 fuel has indicated the occurrence of a mixed Pd-Ag halide particle. One question is whether this phase formed during irradiation in the reactor and was stable or whether the phase formed during the dissolution process from free Ag^+, Pd^{2+}, and I^-. Silver iodide and palladium iodide are only very slightly soluble in water, and would surely precipitate as the fuel dissolves. (Both compounds are sufficiently insoluble to be used for gravimetric iodine analysis [33].) However, hot nitric acid oxidizes iodide to iodine [34,35], which would ultimately partially evaporate as I_2 and be partially converted to iodate through hydrolysis and disproportionation. Silver iodate is more soluble than silver iodide [36]. Silver iodide would not be expected to form as fuel dissolves in strong hot nitric acid, because of oxidation of iodide to iodate. The presence of silver iodide in the nitric acid residue after fuel dissolution implies that silver iodide was present in the fuel before it was dissolved. Furthermore, the variability in the Ag:Pd composition of the phase also suggests that the phase formed in the reactor. If the phase had formed during the dissolution process, the composition would have been more uniform.

The residue from fuel dissolved in ammonium carbonate and hydrogen peroxide had about 700% more iodine than the nitric acid dissolution [24]. This is not surprising, since the ammonium carbonate solution used to dissolve the fuel has a pH of about 10, and at that pH iodide is not oxidized by hydrogen peroxide. If the fission product iodine was present in the fuel as iodide (not I_2 or IO_3^- or other compounds), then it would be expected to precipitate as AgI and PdI_2 in the dissolved fuel solution. However, it would probably precipitate in uniform composition, not as range of Ag:Pd in the precipitate. Plutonium-239 fission yields about as much silver, but more palladium than ^{235}U fission, and as the burnup of the fuel increases and more fission comes from Pu-239, a larger fraction of the iodide precipitate in the fuel should be PdI_2. Early fission product should be largely AgI, and late fission should yield more PdI_2. Then, when the fuel is completely dissolved for analysis, the residue should have a range of both silver and palladium iodide phases, which is what was observed in the SEM analysis.

This is the first microscopic observation of the (Ag,Pd)-halide in spent fuel that explains the neutron activation results reported by Palmores et al. [24]. This study also agrees with Sakuri and coworkers [37] who found evidence of the association of iodine with insoluble residues in SNF. The fission product inventory of Ag, I, and Br from 20 to 50 $MWd \cdot kg^{-1}$ U using ORIGEN2 runs were reported by Gunether et al. [5]. The calculated I:Br ratio is approximately 8.5:1 using values from Gunether et al.; whereas, the experimentally determined I:Br ratio in the halide phase was ~10:1.

5. Conclusion

The approach for modeling radionuclide release from SNF in a geologic repository involves predicting several different physical and chemical processes; however, these processes can be grouped into two parts; the instant release fraction and the matrix release fraction. The instant release fraction is considered to be the radionuclides that are released immediately upon breeching of the outer metal canister containing the nuclear fuel. These radionuclides typically include Xe, Kr, I, and Cs. Based on the neutron activation analysis of these specimens it was established that iodine was retained in high burn-up fuel [11]; however, the mechanism for this retention had not been established. This study clearly demonstrates that iodine is retained within a mixed Ag-Pd halide. This phase was found to be relatively resistant to dissolution in nitric acid and almost completely resistant to dissolution in ammonium carbonate-peroxide solutions. This suggests that iodine from very high burn-up fuels may not be released instantly following fuel failure and may even be released at a rate slower than the matrix contained elements.

Acknowledgements

This work was funded by the Laboratory Directed Research and Development program within the Pacific Northwest National Laboratory (PNNL). PNNL is operated for DOE by Battelle Memorial Institute under contract DE-AC05-76RL01830.

References

[1] R.C. Ewing, Long-term storage of spent nuclear fuel, Nat. Mater. 14 (2015) 252–257.
[2] H. Kleykamp, The chemical state of fission products in oxide fuels, J. Nucl. Mater. 131 (1985) 221–246.
[3] H. Kleykamp, Post-irradiation examinations and composition of the residues from nitric acid dissolution experiments of high burn-up LWR fuel, J. Nucl. Mater. 171 (1990) 181–188.
[4] L.E. Thomas, C.E. Boyer, L.A. Charlot, Microstructural analysis of LWR spent fuels at high burnup, J. Nucl. Mater. 188 (1992) 80–89.
[5] R.J. Guenther, D.E. Blahnik, T.K. Campbell, U.P. Jenquin, J.E. Mendel,

L.E. Thomas, C.K. Thornhill, Characterization of Spent Fuel Approved Testing Material ATM-103, Pacific Northwest Laboratory Report, Richland, 1988. PNL-5109-103.
[6] I.L.F. Ray, H. Thiele, H. Matzke, Transmission electron microscopy study of fission product behavior in high burnup UO_2, J. Nucl. Mater. 188 (1992) 90–95.
[7] D. Cui, V.V. Rondinella, J.A. Fortner, A.J. Kropf, L. Eriksson, D.J. Wronkiewicz, K. Spahiu, Characterization of alloy particles extracted from spent nuclear fuel, J. Nucl. Mater. 420 (2012) 328–333.
[8] T. Wiss, H. Thiele, A. Janssen, D. Papaioannou, V.V. Rondinella, R.J.M. Konings, Recent results of microstructural characterization of irradiated light water reactor fuels using scanning and transmission electron microscopy, JOM 74 (2012) 1390–1395.
[9] J.H. Li, L.T. Kong, B.X. Liu, Proposed definition of microchemical inhomogeneity and application to characterize some selected miscible/immisicle binary metal systems, J. Phys. Chem. B108 (2004) 16071–16076.
[10] E.H. Cordfunke, R.J.M. Konings, The release of fission products from degraded UO_2 fuel: thermochemical aspects, J. Nucl. Mater. 201 (1993) 57–69.
[11] P.C. Burns, R.C. Ewing, A. Navrotsky, Nuclear fuel in a reactor accident, Science 335 (2012) 1184–1188.
[12] R.J.M. Konings, T. Wiss, O. Benes, Predicting material release during a nuclear accident, Nat. Mater. 14 (2015) 247–252.
[13] D. Bard, P. Verger, P. Hubert, Chernobyl, 10 years after: health consequences, Epidemiol. Rev. 19 (2) (1997) 187–204.
[14] Y. Miyake, H. Matsuzaki, T. Fujiwara, T. Saito, T. Yamagata, M. Honda, Y. Muramatsu, Isotope ratio of radioactive iodine (129I/131I) released from Fukushima Daiichi NPP accident, Geochem. J. 46 (2012) 327–333.
[15] J.M. Schwantes, C.R. Orton, R.A. Clark, Analysis of a nuclear accident: fission and activation product releases from the Fukushima Daiihi nuclear facility as remote indicators of source identification, extent of release, and state of damaged spent nuclear fuel, Environ. Sci. Technol. 24 (2012) 8621–8627.
[16] D.G. Abrecht, J.M. Schwantes, Linear free energy correlations for fission product release from the Fukushima Daiichi nuclear accident, Environ. Sci. Technol. 49 (2015) 3158–3166.
[17] N.R. Soelberg, T.G. Garn, M.R. Greenhalgh, J.D. Law, R. Jubin, D.M. Strachan, P.K. Thallapally, Radioactive iodine and krypton control for nuclear fuel reprocessing facilities, Sci. Technol. Nucl. Install. (2013). ID 702496, 12 pgs.
[18] W.J. Gray, Inventories of Iodine-129 and Cesium-137 in the gaps and grain boundaries of LWR spent fuels, Mater. Res. Soc. Symp. Proc. 556 (1999) 487–494.
[19] P.A. Finn, J.C. Hoh, S.F. Wolf, S.A. Slater, J.K. Bates, The release of uranium, technetium, and iodine from spent fuel under unsaturated conditions, Radiochim. Acta 117 (1996) 266–282.
[20] Kienzler, B. & González-Robles, E. 15th Int. Conf. on Environmental Remediation and Radioactive Waste Management Brussels, 09 – 12 Sept. 2013.
[21] S.F. Wolf, D.L. Bowers, J.C. Cunnane, Analysis of high burnup spent nuclear fuel by ICP-MS, J. Radioanal. Nucl. Chem. 263 (2005) 581–586.
[22] E.C. Buck, E.J. Mausolf, B.K. McNamara, C.Z. Soderquist, J.M. Schwantes, Nanostructure of metallic particles in light water reactor used nuclear fuel, J. Nucl. Mater. 461 (2015) 236–243.
[23] B.K. McNamara, E.C. Buck, C.Z. Soderquist, F.N. Smith, E.J. Mausolf, R.D. Scheele, Separation of metallic residues from the dissolution of a high-burnup BWR fuel using nitrogen trifluoride, J.Fluorine Chem. 162 (2014) 1–8.
[24] R.I. Palomares, K.J. Dayman, S. Landsberger, S.R. Biegalski, C.Z. Soderquist, A.J. Casella, M.C. Brady-Raap, J.M. Schwantes, Measuring the noble metal and iodine composition of extracted noble metal phase from used nuclear fuel using instrumental neutron activation analysis, Appl. Radiat. Isot. 98 (2015) 66–70.
[25] C.Z. Soderquist, B.D. Hanson, Dissolution of spent nuclear fuel in carbonate-peroxide Solution, J. Nucl. Mater. 396 (2010) 159–162.
[26] C.Z. Soderquist, A.M. Johnsen, B.K. McNamara, B.D. Hanson, J.W. Chenault, K.J. Carson, S.M. Peper, Dissolution of irradiated commercial UO_2 fuels in ammonium carbonate and hydrogen peroxide, Ind. Eng. Chem. Res. 50 (2011) 1813–1818.
[27] C.A. Schneider, W.S. Rasband, K.W.N.I.H. Eliceiri, Image to ImageJ: 25 years of image analysis, Nat. Meth. 9 (2012) 671–675.
[28] J.P. Mccaffrey, J.-M. Baribeau, A transmission electron microscope (TEM) calibration sample for all magnification, camera constant and image –diffraction pattern rotation calibrations, Microsc. Res. Tech. 32 (1995) 449–454.
[29] D.R.G. Mitchell, DiffTools: electron diffraction software tools for DigitalMicrograph™, Microsc. Res. Tech. 71 (2008) 588–593.
[30] N.W. Ritchie, Spectrum simulation in DTSA-II, Micro. Microanal. 5 (2009) 454–468.
[31] R.W. Grimes, R.G.J. Ball, C.R.A. Catlow, Site preference and binding of iodine and caesium in uranium oxide, J. Phys. Chem. Solids 53 (1992) 75–484.
[32] S.C. Middleburgh, D.M. King, G.R. Lumpkin, Atomic scale modelling of hexagonal structured metallic fission product alloys, R. Soc. open Sci. 2 (2015) 140292.
[33] I.M. Kolthoff, P.J. Elving (Eds.), Treatise on Analytical Chemistry, vol. 7, John Wiley and Sons, New York, 1961, p. 362.
[34] N.V. Sidgewick, The Chemical Elements and Their Compounds, Oxford University Press, London, 1950, p. 1169.
[35] Supplement II, Part 1, Mellor's Comprehensive Treatise on Inorganic and Theoretical Chemistry, Longmans, New York, 1956, p. p 867.
[36] I.M. Kolthoff, P.J. Elving (Eds.), Treatise on Analytical Chemistry, vol. 4, John Wiley and Sons, New York, 1966, p. 17.
[37] T. Sakurai, A. Takahasho, N. Ishikawa, Y. Komaki, The interaction of iodine with insoluble residue in the dissolution of simulated spent-fuel pellets, Nucl. Technol. 94 (1991) 99–107.